

Resonance Kondo Tunneling through a Double Quantum Dot at Finite Bias

M. N. Kiselev¹, K. Kikoin² and L. W. Molenkamp³¹Institut für Theoretische Physik, ³Physikalisches Institut (EP 3),
Universität Würzburg, D-97074 Würzburg, Germany²Ben-Gurion University of the Negev, Beer-Sheva 84105, Israel
(Dated: March 22, 2024)

It is shown that the resonance Kondo tunneling through a double quantum dot (DQD) with even occupation and singlet ground state may arise at a strong bias, which compensates the energy of singlet/triplet excitation. Using the renormalization group technique we derive scaling equations and calculate the differential conductance as a function of an auxiliary dc-bias for parallel DQD described by SO(4) symmetry. We analyze the decoherence effects associated with the triplet/singlet relaxation in DQD and discuss the shape of differential conductance line as a function of dc-bias and temperature.

PACS numbers: 72.10.-d, 72.10.Fk, 72.15.Qm, 05.10.Cc

I. INTRODUCTION

Many fascinating collective effects, which exist in strongly correlated electron systems (metallic compounds containing transition and rare-earth elements) may be observed also in artificial nanosize devices (quantum wells, quantum dots, etc). Moreover, fabricated nanoobjects provide unique possibility to create such conditions for observation of many-particle phenomena, which by no means may be reached in "natural" conditions. Kondo effect (KE) is one of such phenomena. It was found theoretically^{1,2} and observed experimentally^{3,4,5} that the charge-spin separation in low-energy excitation spectrum of quantum dots under strong Coulomb blockade manifests itself as a resonance Kondo-type tunneling through a dot with odd electron occupation N (one unpaired spin $S = 1/2$). This resonance tunneling through a quantum dot connecting two metallic reservoirs (leads) is an analog of resonance spin scattering in metals with magnetic impurities. A Kondo-type tunneling arises under conditions which do not exist in conventional metallic compounds. The KE emerges as a dynamical phenomenon in strong time dependent electric field⁸⁻¹⁰, it may arise at finite frequency under light illumination^{11,12,13}. Even the net zero spin of isolated quantum dot (even N) is not an obstacle for the resonance Kondo tunneling. In this case it may be observed in double quantum dots (DQD) arranged in parallel geometry¹⁴, in T-shaped DQD^{14,15,16}, in two-level single dots^{17,18} or induced by strong magnetic field^{9,20,21,22} whereas in conventional metals magnetic field only suppresses the Kondo scattering. The latter effect was also discovered experimentally^{23,24,25}.

One of the most challenging options in Kondo physics of quantum dots is the possibility of controlling the Kondo effect by creating the non-equilibrium reservoir of fermionic excitations by means of strong bias $eV > T_K$ applied between the leads²⁶ (T_K is the equilibrium Kondo temperature which determines the energy scale of low-energy spin excitations in a quantum dot). However, in this case the decoherence effects may prevent the formation of a full scale Kondo resonance (see, e.g. dis-

cussion in Refs. 27,28,29). It was argued in recent disputes that the processes, associated with the finite current through a dot with odd N may destroy the coherence on an energy scale T_K and thus prevent formation of a ground state Kondo singlet, so that only the weak coupling Kondo regime is possible in strongly non-equilibrium conditions.

In the present paper we discuss Kondo tunneling through DQD with even N , whose ground state is a spin singlet $\uparrow\downarrow$. It will be shown that the Kondo tunneling through excited triplet state $\uparrow\uparrow$ arises at finite eV . In this case the ground state is stable against any kind of spin-flip processes induced by external current, the decoherence effects develop only in the intermediate (virtual) triplet state, and the estimates of decoherence rate should be revisited.

As was noticed in Ref. 15, quantum dots with even N possess the dynamical symmetry SO(4) of spin rotator in the Kondo tunneling regime, provided the low-energy part of excitation spectrum is formed by a singlet-triplet (ST) pair, and all other excitations are separated from the ST manifold by a gap noticeably exceeding the tunneling rate. A DQD with even N in a side-bound (T-shape) configuration where two wells are coupled by the tunneling v and only one of them (say, L) is coupled to metallic leads (L;R) is a simplest system satisfying this condition¹⁵. Such system was realized experimentally in Ref.30. Novel features introduced by the dynamical symmetry in Kondo tunneling are connected with the fact that unlike the case of conventional SU(2) symmetry of spin vector S , the SO(4) group possesses two generators S and P . The latter vector describes transitions between singlet and triplet states of spin manifold (this vector is an analog of Runge-Lenz vector describing the hidden symmetry of hydrogen atom). As was shown in Ref. 14, this vector alone is responsible for Kondo tunneling through quantum dot with even N induced by external magnetic field.

Another manifestation of dynamical symmetry peculiar to DQDs with even N is revealed in this paper. It is shown that in the case when the ground state is singlet

Si and the S/T gap T_K , a Kondo resonance channel arises under a strong bias eV comparable with T_K . The channel opens at $eV > T_K$, and the tunneling is determined by the non-diagonal component $J_{ST} = \hbar t^\dagger j^\dagger j^\dagger$ of effective exchange induced by the electron tunneling through DQD (see Fig. 1 (right panel)).

II. COTUNNELING HAMILTONIAN OF T-SHAPED DQD

The basic properties of symmetric DQD occupied by even number of electrons $N = 2n$ under strong Coulomb blockade in each well are manifested already in the simplest case $n = 1$, which is considered below. Such DQD is an artificial analog of a hydrogen molecule H_2 . If the inter-well Coulomb blockade Q is strong enough, one has $N = n_l + n_r$; $n_l = n_r = 1$; the lowest states of DQD are singlet and triplet and the next levels are separated from ST pair by a charge transfer gap Q . We assume that both wells are neutral at $n_{l,r} = 1$. Then the effective inter-well exchange I responsible for the singlet-triplet splitting arises because of tunneling v between two wells, $I = v^2/Q =$. It is convenient to write the effective spin Hamiltonian of isolated DQD in the form

$$H_d = E_S \mathbf{S} \cdot \mathbf{I} + E_T \mathbf{T} \cdot \mathbf{I} + E_X \mathbf{X} \cdot \mathbf{X} \quad (1)$$

where $\mathbf{X} = j^\dagger i \mathbf{I} j$ is a Hubbard configuration change operator (see, e.g.,³¹), $E_T = E_S +$, $=$; 0 are three projections of $S = 1$ vector. Two other terms completing the Anderson Hamiltonian, which describes the system shown in Fig.1 (left panel), are

$$H_b + H_t = \sum_k \sum_{\sigma} c_{k\sigma}^\dagger c_{k\sigma} + \sum_k \sum_{\sigma} W c_{k\sigma}^\dagger c_{k\sigma} + H_{\text{lead}} \quad (2)$$

The first term describes metallic electrons in the leads and the second one stands for tunneling between the leads and the DQD. Here $L; R$ marks electrons in the left and right lead, respectively, the bias eV is applied to the left lead, so that the chemical potentials are $\mu_L = \mu_R + eV$, W is the tunneling amplitude for the well (left), j_i are one-electron states of DQD, which arises after escape of an electron with spin projection from DQD in a state j_i . We solve the problem in a Schrieffer-Wolff (SW) limit³¹, when the activation energies $E_j - E_F$ and Coulomb blockade energy Q are essentially larger than the tunneling rate Γ , and charge fluctuations are completely suppressed both in the ground and excited state of DQD. In this limit one may start with the SW transformation, which projects out charge excitations. We confine ourselves with the bias $eV > T_K$, where D is the width of the electrons in

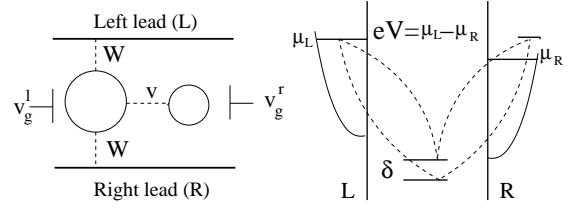


FIG. 1: Left panel: Double quantum dot in a side-bound configuration. Right panel: cotunneling processes in biased DQD responsible for the resonance Kondo tunneling.

the leads, so the leads are considered in the SW transformation as two independent quasi-equilibrium reservoirs (cf.^{8,9}). As is shown in Ref.¹⁵, the SW transformation being applied to a spin rotator results in the following effective spin Hamiltonian

$$H_{\text{int}} = \sum_{\sigma} [(J^T T_0 S + J^S T_0 P) s_{\sigma} + J^{SS} X^S s_{\sigma}] \quad (3)$$

Here $s_{\sigma} = \sum_{kk^0} c_{k\sigma}^\dagger c_{k^0\sigma}^\dagger$, $n_{\sigma} = \sum_{kk^0} c_{k\sigma}^\dagger c_{k^0\sigma}$, $\hat{\sigma}$, \hat{I} are the Pauli matrices and unity matrix respectively. The effective exchange constants are

$$J_{\sigma} = \frac{W}{2} \frac{1}{E_S - 2} + \frac{1}{E_S - 2} \quad :$$

In this approximation the small differences between singlet and triplet states are neglected. Besides, $J_{\sigma} = I$ in real DQD.

Two vectors S and P with spherical components

$$\begin{aligned} S^+ &= \frac{1}{2} X^{10} + X^{01}; \quad S^- = \frac{1}{2} X^{01} + X^{10}; \\ S_z &= X^{11} - X^{1-1}; \quad P_z = X^{0S} + X^{S0}; \\ P^+ &= \frac{1}{2} X^{1S} - X^{S1}; \quad P^- = \frac{1}{2} X^{S1} - X^{1S}; \end{aligned} \quad (4)$$

obey the commutation relations of o_4 algebra

$$[S_j; S_k] = ie_{jkl} S_l; \quad [P_j; P_k] = ie_{jkl} S_l; \quad [P_j; S_k] = ie_{jkl} P_l$$

($j; k; l$ are Cartesian coordinates, e_{jkl} is a Levi-Civita tensor). These vectors are orthogonal, $S \cdot P = 0$; and the Casimir operator is $S^2 + P^2 = 3$. Thus, the singlet state is involved in spin scattering via the components of the vector P .

We use SU(2)-like semi-fermionic representation for S operators^{32,33}

$$\begin{aligned} S^+ &= \frac{1}{2} (f_0^\dagger f_{-1} + f_1^\dagger f_0); \quad S^- = \frac{1}{2} (f_{-1}^\dagger f_0 + f_0^\dagger f_1); \\ S_z &= f_1^\dagger f_1 - f_{-1}^\dagger f_{-1}; \end{aligned} \quad (5)$$

where $f_{\pm 1}$ are creation operators for fermions with spin "up" and "down" respectively, whereas f_0 stands for spinless fermion^{32,33}. This representation can be generalized for SO(4) group by introducing another spinless

fermion f_s to take into consideration the singlet state. As a result, the P -operators are given by the following equations:

$$P^+ = \frac{P}{2} (\bar{f}_1^y f_s \quad \bar{f}_s^y f_1); \quad P^- = \frac{P}{2} (f_s^y f_1 \quad f_1^y f_s);$$

$$P^z = (\bar{f}_0^y f_s + f_s^y f_0): \quad (6)$$

The Casimir operator $S^2 + P^2 = 3$ transforms to the local constraint

$$\sum_{\mathbf{k}} f^y f = 1:$$

$$= ;0;s$$

The normal form of the spin cotunneling Hamiltonian is

$$H_{\text{int}} = \sum_{\mathbf{k}\mathbf{k}'; \quad \sigma=L,R} J^S_{\sigma} \bar{f}_s^y f_s c_{\mathbf{k}}^y c_{\mathbf{k}'}^y c_{\mathbf{k}'}^{\dagger} c_{\mathbf{k}}^{\dagger} \quad (7)$$

$$+ \sum_{\mathbf{k}\mathbf{k}'; \quad \sigma=L,R} J^T_{\sigma} \hat{S}_{\sigma}^d + J^{ST}_{\sigma} \hat{P}_{\sigma}^d c_{\mathbf{k}}^y c_{\mathbf{k}'}^y f^y f_0$$

where \hat{S}^d and \hat{P}^d ($d=x,y,z$) are 4×4 matrices defined by relations (4) – (6) and $J^S = J^{SS}$, $J^T = J^{TT}$ and J^{ST} are singlet, triplet and singlet-triplet coupling SW constants, respectively.

The cotunneling in the ground singlet state is described by the first term of the Hamiltonian (7), and no spin flip processes accompanying the electron transfer between the leads emerge in this state. However, the last term in (7) links the singlet ground state with the excited triplet and opens a Kondo channel. In equilibrium this channel is ineffective, because the incident electron should have the energy to be able to initiate spin-flip processes. We will show in the next section that the situation changes radically, when strong enough external bias is applied.

III. KONDO SINGULARITY IN TUNNELING THROUGH DQD AT FINITE BIAS

We deal with the case, which was not met in the previous studies of non-equilibrium Kondo tunneling. The ground state of the system is singlet, and the Kondo tunneling in equilibrium is quenched at $T = 0$. Thus, the elastic Kondo tunneling arises only provided T_K in accordance with the theory of two-impurity Kondo effect^{5,35}. However, the energy necessary for spin flip may be donated by external electric field eV applied to the left lead, and in the opposite limit $T_K \rightarrow 0$ the elastic channel emerges at $eV = T_K$. The processes responsible for resonance Kondo cotunneling at finite bias are shown in Fig. 1 (left panel).

In conventional spin $S = 1/2$ quantum dots the Kondo regime out of equilibrium is affected by spin relaxation and decoherence processes, which emerge at $eV \sim T_K$ (see, e.g.,^{9,27,28,29}). These processes appear in the same order as Kondo co-tunneling itself, and one should use

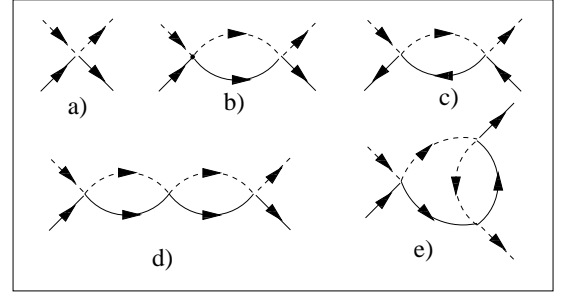


FIG. 2: Leading (b,d) and next to leading (c,e) parquet diagrams determining renormalization of J^S (a). Solid lines denote electrons in the leads. Dashed lines stand for electrons in the dot.

the non-equilibrium perturbation theory (e.g., Keldysh technique) to take them into account in a proper way. In our case these effects are expected to be weaker, because the nonzero spin state is involved in Kondo tunneling only as an intermediate virtual state arising due to S/T transitions induced by the second term in the Hamiltonian (3), which contains vector P . The non-equilibrium repopulation effects in DQD are weak as well (see next section, where the nonequilibrium effects are discussed in more details).

Having this in mind, we describe Kondo tunneling through DQD at finite eV within the quasi-equilibrium perturbation theory in a weak coupling regime (cf. the quasi-equilibrium approach to description of decoherence rate at large eV in Ref. 27). To develop the perturbative approach for $T > T_K$ we introduce the temperature Green's functions (GF) for electrons in a dot, $G(\omega) = \langle T f(\omega) f^\dagger(0) \rangle$; and GF for the electrons in the left (L) and right (R) lead, $G_{L,R}(\mathbf{k}; \omega) = \langle T c_{L,R}(\mathbf{k}; \omega) c_{L,R}^\dagger(\mathbf{k}; 0) \rangle$. Performing a Fourier transformation in imaginary time for bare GF's, we come to following expressions:

$$G_K^0(\omega) = (i\omega - \epsilon_K + \epsilon_{L,R})^{-1};$$

$$G^0(\omega_m) = (i\omega_m - E_T)^{-1}; \quad \omega_m = 2\pi T(m + 1/2)$$

$$G_S^0(\omega) = (i\omega - E_S)^{-1}; \quad (8)$$

with $\epsilon_K = 2T(n + 1/2)$ and $\omega_m = 2T(m + 1/2)$ ^{32,33}. The first leading and next to leading parquet diagrams are shown on Fig 2. Corrections to the singlet vertex $\langle T f^\dagger(0) f(\omega) \rangle$ are calculated using an analytical continuation of GF's to the real axis ω and taking into account the shift of the chemical potential in the left lead. Since the electron from the left lead tunnels into the empty state in the right lead separated by the energy eV , we have to put $\epsilon_L = eV$, $\epsilon_R = 0$ in the final expression for $\langle T f^\dagger(0) f(\omega) \rangle$. Thus, unlike conventional Kondo effect we deal with the vertex at finite frequency ω similarly to the problem considered in Ref. 27. We assume that the

leads remain in equilibrium under applied bias and neglect the relaxation processes in the leads ("hot" leads). In a weak coupling regime $T > T_K$ the leading non-Born contributions to the tunnel current are determined by the diagrams of Fig. 2b-e.

The effective vertex shown in Fig. 2b is given by the following equation

$$\Gamma_{LR}^{(2b)}(\omega) = J_{LL}^{ST} J_{LR}^{TS} \sum_k \frac{1}{\omega - \epsilon_k} \frac{f(\epsilon_k)}{\epsilon_k + \epsilon_L} \quad (9)$$

Changing the variable ϵ_k for $\epsilon_k = \epsilon_V$ one finds that

$$\Gamma_{LR}^{(2b)}(\omega = \epsilon_V) = J_{LL}^{ST} J_{LR}^{TS} \ln(D = \max(\epsilon_V, T)); T g) \quad (10)$$

Here $D = \frac{V_F}{\rho}$ is a cutoff energy determining effective bandwidth, ρ is a density of states on a Fermi level and $f(\omega)$ is the Fermi function. Therefore, under condition $|\epsilon_V| \ll \max(\epsilon_V, T)$ this correction does not depend on ϵ_V and becomes quasielastic.

Unlike the diagram Fig. 2b, its "parquet counterpart" term Fig. 2c contains $\epsilon_V + T$ in the argument of the Kondo logarithm:

$$\Gamma_{LR}^{(2c)}(\omega) = J_{LL}^{ST} J_{LR}^{TS} \sum_k \frac{f(\epsilon_k)}{\epsilon_k + \epsilon_L + \epsilon_V} \quad (10)$$

At $\epsilon_V = T$ this contribution is estimated as

$$\Gamma_{LR}^{(2c)}(\epsilon_V) = J_{LL}^{ST} J_{LR}^{TS} \ln(D = (\epsilon_V + T)); T g) \quad (11)$$

Similar estimates for diagram of Fig. 2d and 2e give

$$\Gamma_{LR}^{(2d)}(\omega) = J_{LL}^{ST} J_{LL}^T J_{LR}^{TS} \ln^2(D = \max(\omega, T)); T g) \quad (12)$$

$$\Gamma_{LR}^{(2e)}(\omega) = J_{LL}^{ST} J_{LL}^T J_{LR}^{TS} \ln^2(D = \max(\omega, T)); T g) \quad (13)$$

$$\ln(D = \max(\omega, T)); T g) \quad (11)$$

Then $\Gamma_{LR}^{(2e)}(\omega) = \Gamma_{LR}^{(2d)}(\omega)$ at $\omega = T$.

Thus, the Kondo singularity is restored in non-equilibrium conditions where the electrons in the left lead acquire additional energy in external electric field, which compensates the energy loss in a singlet-triplet excitation. The leading sequence of most divergent diagrams degenerates in this case from a parquet to a ladder series.

Following the poor man's scaling approach, we derive the system of coupled renormalization group (RG) equations for (7). The equations for LL co-tunneling are:

$$\frac{dJ_{LL}^T}{d \ln D} = (J_{LL}^T)^2; \quad \frac{dJ_{LL}^{ST}}{d \ln D} = J_{LL}^{ST} J_{LL}^T; \quad (12)$$

The scaling equations for J_{LR} are as follows:

$$\frac{dJ_{LR}^T}{d \ln D} = J_{LL}^T J_{LR}^T; \quad \frac{dJ_{LR}^{ST}}{d \ln D} = J_{LL}^{ST} J_{LR}^T; \quad (13)$$

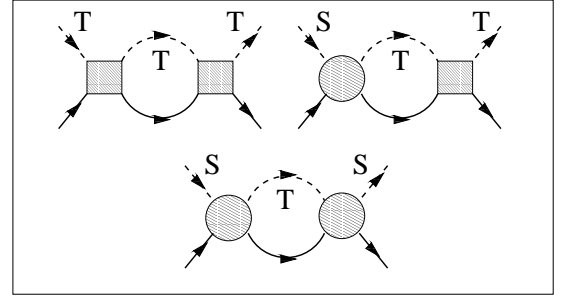


FIG. 3: Irreducible diagrams contributing to RG equations. Hatched boxes and circles stand for triplet-triplet and singlet-triplet vertices respectively. Notations for lines are the same as in Fig. 2

$$\frac{dJ_{LR}^S}{d \ln D} = \frac{1}{2} J_{LL}^{ST} J_{LR}^{TS} + \frac{1}{2} J_{LL}^{ST} J_{LR}^{TS} : \quad (13)$$

One-loop diagrams corresponding to the poor man's scaling procedure are shown in Fig. 3. To derive these equations we collected only terms $(J^T)^n \ln^{n+1}(D=T)$ neglecting contributions containing $\ln D = (\epsilon_V)$. The analysis of RG equations beyond the one loop approximation will be published elsewhere. The solution of the system (13) reads as follows:

$$J_{LR}^T;_0 = \frac{J_0^T}{1 - J_0^T \ln(D=T)}; \quad J_{LR}^{ST};_0 = \frac{J_0^{ST}}{1 - J_0^{ST} \ln(D=T)};$$

$$J_{LR}^S = J_0^S - \frac{3}{4} (J_0^{ST})^2 \frac{\ln(D=T)}{1 - J_0^T \ln(D=T)}; \quad (14)$$

Here $\omega = L, \omega_0 = L, R$. One should note that the Kondo temperature is determined by triplet-triplet processes only in spite of the fact that the ground state is singlet. One finds from (14) that $T_K = D \exp[1/(J_0^T)]$. This temperature is noticeably smaller than the "equilibrium" Kondo temperature T_{K0} , which emerges in tunneling through triplet channel in the ground state, namely $T_K = T_{K0}^2/D$. The reason for this difference is the reduction of usual parquet equations for T_K to a simple ladder series. In this respect our case differs also from conventional Kondo effect at strong bias²⁷, where the non-equilibrium Kondo temperature $T_{K0} = \epsilon_V$ arises. In our model the finite bias does not enter T_K because of the compensation ϵ_V in spite of the fact that we take the argument $\omega = \epsilon_V$ in the vertex (9). The differential conductance $G(\epsilon_V; T) = G_0 \frac{J_{LR}^{ST}}{J_{LR}^T}$ (cf. Ref. 37) is the universal function of two parameters $T = T_K$ and $\epsilon_V = T_K$, $G_0 = e^2 = \sim$:

$$G = G_0 \ln^2(\max(\epsilon_V, T)/T_K) \quad (15)$$

Its behavior as a function of bias and temperature is shown in Fig. 4. It is seen from this picture that the resonance tunneling "ashes" at $\epsilon_V = T_K$ and dies away out of this resonance. In this picture the decoherence effects are not taken into account, and its stability against various non-equilibrium corrections should be checked.

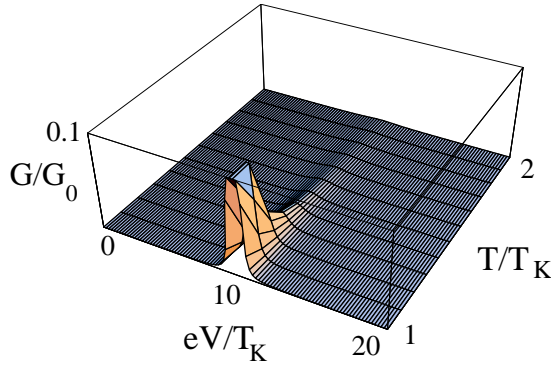


FIG. 4: The Kondo conductance as a function of dc-bias $eV = T_K$ and $T = T_K$. The singlet-triplet splitting $\Delta = T_K = 10$.

IV. DECOHERENCE EFFECTS

We analyze now the decoherence rate $\sim \omega_d$ associated with T/S transition relaxation induced by cotunneling. The calculations are performed in the same order of the perturbation theory as it has been done for the vertex renormalization (see Figs. 2 and 3). The details of the calculation scheme are presented in Appendix.

To estimate the decoherence effects, one should calculate the decay of the triplet state or in other terms to find the imaginary part of the retarded self energy of triplet semi-fermion propagators at actual frequency [see discussion before Eq. (9)], $\sim \omega_d = 2\text{Im} \Sigma^R_T(\omega)$. The 2nd and 3rd order diagrams determining $\sim \omega_d$ are shown in Fig. 5 (a-d). Two leading terms given by the diagrams of Fig. 5 (a,b) describe the damping of triplet excitation due to its inelastic relaxation to the ground singlet state. These terms are calculated in Appendix (see Eqs. (A.8), (A.10)). One finds from these equations that the relaxation rate associated with ST transition is

$$\Gamma_d^{ST} = J^{ST} = D^2 \max[\omega; \Delta; T_K] \quad (16)$$

It should be noted that for corrections associated with LL (RR) diagrams (Fig. 5a), describing co-tunneling processes on a left (right) lead, the use of quasi-equilibrium technique is fully justified when the leads themselves are in thermal equilibrium. We are interested in the zero frequency damping at resonance $eV = \Delta$. Neglecting the small difference between J^T and J^{ST} (see¹⁵), we also take $J^T = J^{ST} = J$. Thus the T \rightarrow S spin relaxation effect (16) does not contain logarithmic enhancement factor in the lowest order. It is estimated as

$$\Gamma_d^{ST}(\omega) = (J=D^2) J^3 = D^2 : \quad (17)$$

The repopulation of triplet state as a function of external bias is controlled by the occupation number for triplet state modified by the bias eV . The latter, in turn, depends on the modified exchange splitting given by solution of the equation

$$\Delta = \text{Re} \Sigma^R(\omega; eV; T) : \quad (18)$$

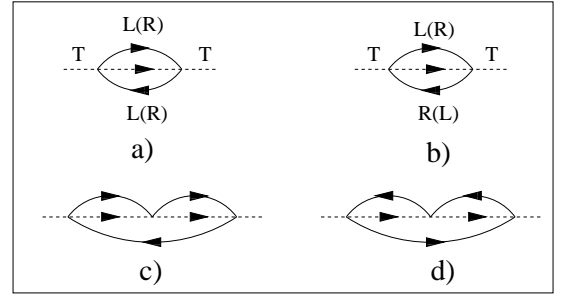


FIG. 5: Leading diagrams (a-d) for $\sim \omega_d$ (see text). Dashed line in the self-energy part stands for the singlet state of a two-electron configuration in the dot.

The $\text{Re} \Sigma^R$ (Fig. 5 (a,b)) is given by

$$\text{Re} \Sigma_{TST}^{R(2)}(\omega; eV; T) = a_2 \frac{J^2}{D} \ln \frac{D}{\max[\omega; eV; T]} \quad (19)$$

where $a_2 \approx 1$ is a numerical coefficient. As it is seen, the perturbative equation for $\text{Re} \Sigma^R$ is beyond the scope of leading-log approximation. As a result, $\omega_d(eV)$ and repopulation of the triplet state is exponentially small. The corresponding factor in the occupation number is

$$P_t(eV) = \exp(-\omega_d(eV)/T) \quad (20)$$

The effects of repopulation become important only at $eV \sim \Delta$ when $\omega_d \sim \Delta$. In that case the quasi-equilibrium approach is not applicable and one should start with the Keldysh formalism^{27,28}. This regime is definitely not realized in conditions considered above.

Next 2nd order contribution is the damping of triplet state itself given by Eqs. (A.12), (A.14). It is seen from these equations that this damping is of threshold character:

$$\Gamma_d^{TT} = (J=D^2) \theta(\omega - \Delta) \theta(\omega - T) ; \quad (21)$$

where $\theta(\omega)$ is a Heaviside step function. These processes emerge only at $\omega > \Delta$, so unlike the conventional case²⁷ they are not dangerous.

Corresponding contribution to $\text{Re} \Sigma^R$ casts the form

$$\text{Re} \Sigma_{TTT}^{R(2)} = b_2 \frac{J^2}{D} \theta(\omega - \Delta) \ln \frac{D}{\max[\omega - \Delta; T]} ; \quad (22)$$

where $b_2 \approx 1$.

Next, one has to check whether the higher order logarithmic corrections modify the estimate (17). These corrections start with the 3-rd order terms shown in Fig. 5 (c,d). Straightforward calculations lead to $\omega_d(J=D^2)^3 \ln(D/\omega)$ correction (see the first term Eq. A.23). This leading term like the 2-nd order term originates from T \rightarrow S spin relaxation processes. All other

contributions are either of threshold character, or vanish at $\Gamma \rightarrow 0$. As a result, the estimate

$$\sim \frac{1}{D} \left(\frac{J}{\Gamma} \right)^2 [1 + O(J \ln D / \Gamma)]$$

holds. The topological structure (sequence of intermediate singlet and triplet states and cotunneling processes in the left and right lead) in perturbative corrections for the triplet selfenergy part is different from those for the singlet-singlet vertex (see Appendix). Namely, the leading (ladder) diagrams for the vertex contain maximal possible number of intermediate triplet states, whereas the higher order non-threshold log-diagrams for the selfenergy part must contain at least one intermediate singlet state. As it is seen from the Appendix (Eq.(A.18)–(A.23)), the higher order contributions to $\text{Im } \Sigma_T(\Gamma)$ are not universal and the coefficients in front of log have sophisticated frequency dependence. As a result, the perturbative series for triplet selfenergy part can not be collected in parquet structures and remain beyond the leading-log approximation discussed in the Section III. There is no strong enhancement of the 2nd order term in SO(4) spin rotator model in contrast to SU(2) case discussed in²⁷. As was pointed out above, the main reason for differences in estimates of coherence rate is that in case of QD with odd N , the Kondo singlet develops in the ground state of the dot, and decoherence frustrate this ground state. In DQD with even N the triplet spin state arises only as a virtual state in cotunneling processes, and our calculations demonstrate explicitly that decoherence effects in this case are essentially weaker.

The 3-rd order correction to Re Σ is given by

$$\text{Re } \Sigma^{(3)}(\Gamma) = \frac{J}{D} \ln^2 \frac{D}{\Gamma} \quad (23)$$

(see Appendix). This correction also remains beyond the leading-log approximation.

Thus we conclude that the decoherence effects are not destructive for Kondo tunneling through T-shaped DQD, i.e. the $\Gamma_K \sim \frac{1}{D}$ is valid provided

$$(\Gamma/D)^2 \ll \Gamma_K \quad (24)$$

This interval is wide enough because $\Gamma/D \ll 1$ in the Anderson model.

The same calculation procedure may be repeated in Keldysh technique. It is seen immediately that in the leading-log approximation the off-diagonal terms in Keldysh matrix are not changed in comparison with equilibrium distribution functions because of the same threshold character of repopulation processes, so in the leading approximation the key diagram Fig. 5b (determining L-R current through the dot) calculated in Keldysh technique remains the same as (A.8)–(A.10).

In fact, repopulation effects result in asymmetry of the Kondo-peak similar to that in Ref. 28 due to the threshold character of $\text{Im } \Sigma_{TT}$ (see Appendix). This asymmetry becomes noticeable at $\Gamma \sim \Gamma_K$, where our quasi-equilibrium

approach fails, but this region is beyond our interest, because the bias-induced Kondo tunneling is negligible at large biases (see Fig. 4).

V. CONCLUDING REMARKS

We have shown in this paper that the tunneling through DQD with even N with singlet ground state and triplet excitation divided by the energy gap Γ_K from the singlet state exhibits a peak in differential conductance at $eV = \Gamma_K$ (Fig. 4). This result is in striking contrast with the zero bias anomaly (ZBA) at $eV = 0$ which arises in the opposite limit, $\Gamma \ll \Gamma_K$. In the latter case the Kondo screening is quenched at energies less than Γ , so the ZBA has a form of a dip in the Kondo peak (see¹⁸ for detailed explanation of this effect).

In this case strong external bias initiates the Kondo effect in DQD, whereas in a conventional situation (QD with odd N spin 1/2 in the ground state) strong enough bias is destructive for Kondo tunneling. We have shown that the principal features of Kondo effect in this specific situation may be captured within a quasiequilibrium approach. The scaling equations (13), (14) can also be derived in Schwinger-Keldysh formalism (see Refs. 28,33) by applying the "poor man's scaling" approach directly to the dot conductance⁸.

Of course, our RG approach is valid only in the weak coupling regime. Although in our case the limitations imposed by decoherence effects are more liberal than those existing in conventional QD, they apparently prevent the full formation of the Kondo resonance. To clarify this point one has to use a genuine non-equilibrium approach, and we hope to do it in forthcoming publications.

One should mention yet another possible experimental realization of resonance Kondo tunneling driven by external electric field. Applying the alternate field $V = V_{ac} \cos(\omega t)$ to the parallel DQD, one takes into consideration two effects, namely (i) enhancement of Kondo conductance by tuning the amplitude of ac-voltage to satisfy the condition $j_e V_{ac} \approx \Gamma_K$ and (ii) spin decoherence effects due to finite decoherence rate⁸. One can expect that if the decoherence rate $\sim \Gamma_K$;

$$G_{\text{peak}} = G_0 \ln^2(\Gamma \sim \Gamma_K) \quad (25)$$

whereas in the opposite limit $\Gamma \ll \Gamma_K$,

$$G_{\text{peak}} = \overline{G(V_{ac} \cos[\omega t])} \quad (26)$$

is averaged over a period of variation of ac bias. In this case the estimate (15) is also valid.

In conclusion, we have provided the first example of Kondo effect, which exists only in non-equilibrium conditions. It is driven by external electric field in tunneling through a quantum dot with even number of electrons, when the low-lying states are those of spin rotator. This is not too exotic situation because as a

rule, a singlet ground state implies a triplet excitation. If the ST pair is separated by a gap from other excitons, then tuning the dc-bias in such a way that applied voltage compensates the energy of triplet excitation, one reaches the regime of Kondo peak in conductance. This theoretically predicted effect can be observed in dc- and ac-biased double quantum dots in parallel geometry.

ACKNOWLEDGMENTS

This work is partially supported (MK) by the European Commission under LF project: Access to the Weizmann Institute Submicron Center (contract num-

ber: HPRIC-T-1999-00069). The authors are grateful to Y. Avishai, A. Finkelstein, A. Rosch and M. Heiblum for numerous discussions. The financial support of the Deutsche Forschungsgemeinschaft (SFB-410) is acknowledged. The work of KK is supported by ISF grant.

APPENDIX

We calculate perturbative corrections for $\langle ! \rangle$ by performing analytical continuation of $\langle !_n \rangle$ into upper halfplane of $!$. The parameter of perturbation theory is J^{-1} where ρ denotes the density of states for conduction electrons at the Fermi surface.

The 2-nd order self energies have following structure (the indices T and ST in exchange vertices are temporarily omitted):

$$\langle !_n \rangle^{(2)} = J^2 T^2 \sum_{!_1 !_2 k_1 k_2}^X G^0(!_1; k_1) G^0(!_2; k_2) G^0(!_n + !_1 + !_2) \quad (A.1)$$

The Green functions (GF) are defined in Eq. (8). Performing summation over Matsubara frequencies $!_1; !_2$ and replacing the summation over $k_1; k_2$ by integration

over $!_1; !_2$ in accordance with standard procedure, we come to following expression

$$\langle !_n \rangle^{(2)} = \frac{1}{2} (J_D)^2 \sum_D^Z d_1 \sum_D^Z d_2 \frac{\tanh \frac{1}{2T}}{!_n + !_2} \frac{\tanh \frac{2}{2T}}{!_1} \frac{\tanh \frac{1}{2T}}{S;T} \frac{\tanh \frac{2}{2T}}{!_n + !_2} \quad (A.2)$$

Here we assumed that conduction electron's band has a width $W = 2D_F - D$ and $\epsilon = 1=D$ in order to simplify our calculations. This assumption is sufficient for logarithmic accuracy of our theory. The Lagrange multipliers $S;T$ are different for singlet (triplet) GF, namely $S = E_S$ and $T = E_T + iT=3$

To account for decoherence effects in the same order of perturbation theory as we have done for the vertex corrections, we focus on the self-energy (SE) part of

triplet GF. This SE has to be plugged in back to a semi-fermionic propagator to provide a self-consistent treatment of the problem. We denote the self-energy parts associated with singlet/triplet and triplet/triplet transitions as T_{ST} and T_{TT} respectively.

To prevent double occupancy of singlet/triplet states we take the limit $\lim_{T \rightarrow 0} \text{Re}[S;T] = T$ in the numerator of Eq. (A.2). As a result, Eq. (A.2) casts the form

$$\langle !_n \rangle^{(2)} = (J_D)^2 \sum_D^Z d_1 \sum_D^Z d_2 \frac{n(!_2)(1 - n(!_1))}{!_n + !_2} \frac{1}{!_1} \frac{1}{S;T} \quad (A.3)$$

Since all spurious states are "frozen out" we can put $\tilde{S} = 0$ and $\tilde{T} = E_T - E_S$ in denominator (in the latter

case we perform a shift $\tilde{T} = T - iT=3$) and proceed with the analytical continuation $!_n \rightarrow ! + i0^+$. Without

loss of generality we assume $\epsilon \neq 0$. As a result, we get for retarded (R) self-energies

$$\text{Im } \Sigma_{TST}^{(2)R}(\epsilon) = J^{ST} \int_0^{Z_D} d\epsilon_1 \int_0^{Z_D} d\epsilon_2 n(\epsilon_2) (1 - n(\epsilon_1)) (\epsilon + \epsilon_2 - \epsilon_1) \quad (\text{A.4})$$

$$\text{Re } \Sigma_{TST}^{(2)R}(\epsilon) = J^{ST} \int_0^{Z_D} d\epsilon_1 \int_0^{Z_D} d\epsilon_2 n(\epsilon_2) (1 - n(\epsilon_1)) P \frac{1}{\epsilon + \epsilon_2 - \epsilon_1} \quad (\text{A.5})$$

$$\text{Im } \Sigma_{TTT}^{(2)R}(\epsilon) = J^T \int_0^{Z_D} d\epsilon_1 \int_0^{Z_D} d\epsilon_2 n(\epsilon_2) (1 - n(\epsilon_1)) (\epsilon + \epsilon_2 - \epsilon_1) \quad (\text{A.6})$$

$$\text{Re } \Sigma_{TTT}^{(2)R}(\epsilon) = J^T \int_0^{Z_D} d\epsilon_1 \int_0^{Z_D} d\epsilon_2 n(\epsilon_2) (1 - n(\epsilon_1)) P \frac{1}{\epsilon + \epsilon_2 - \epsilon_1} \quad (\text{A.7})$$

where P denotes the principal value of the integral.

We start with discussion of selfenergy parts determining the spin relaxation due to $T \rightarrow S$ transitions shown

in Fig. 5(a,b). Assuming $T \ll D$ and neglecting temperature corrections at low temperatures $T \ll T$, we get

$$\text{Im } \Sigma_{TST}^{(2)R}(\epsilon) = J^{ST} \int_0^{Z_D} d\epsilon_1 \int_0^{Z_0} d\epsilon_2 (\epsilon + \epsilon_2 - \epsilon_1) = J^{ST} \int_0^{Z_0} d\epsilon_1 J^{ST} \int_0^{Z_0} d\epsilon_2 \quad (\text{A.8})$$

$$\text{Re } \Sigma_{TST}^{(2)R}(\epsilon) = J^{ST} \int_0^{Z_D} d\epsilon_1 \int_0^{Z_0} d\epsilon_2 P \frac{1}{\epsilon + \epsilon_2 - \epsilon_1} = J^{ST} \int_0^{Z_0} d\epsilon_1 \ln \frac{D}{\epsilon} \quad (\text{A.9})$$

In the opposite limit $T \gg D$

$$\text{Im } \Sigma_{TST}^{(2)R}(\epsilon) = J^{ST} T; \quad (\text{A.10})$$

$$\text{Re } \Sigma_{TST}^{(2)R}(\epsilon) = J^{ST} T \ln \frac{D}{2T} \quad (\text{A.11})$$

where $\ln = C = 0.577...$ is the Euler constant.

Next we turn to calculation of the triplet level damping due to TT relaxation processes (Fig. 5a,b). According to the Feynman codex, we can put $E_S = 0$ at the first stage since the population of triplet excited state is controlled by finite level splitting. The contribution from diagram Fig. 5a is given by

$$\text{Im } \Sigma_{TTT}^{(2)R} = \text{Im } \Sigma_{TTT}^{(2)R} J_0^T \int_0^{Z_0} d\epsilon_1 \int_0^{Z_0} d\epsilon_2 \quad (\text{A.12})$$

$$\text{Re } \Sigma_{TTT}^{(2)R} = \text{Re } \Sigma_{TTT}^{(2)R} J_0^T \int_0^{Z_0} d\epsilon_1 \int_0^{Z_0} d\epsilon_2 \ln \frac{D}{\epsilon} \quad (\text{A.13})$$

Similarly for Fig. 5b,

$$\text{Im } \Sigma_{TTT}^{(2)R} = \text{Im } \Sigma_{TTT}^{(2)R} J_0^T \int_0^{Z_0} d\epsilon_1 \int_0^{Z_0} d\epsilon_2 \quad (\text{A.14})$$

and, with logarithmic accuracy

$$\text{Re } \Sigma_{TTT}^{(2)R} = \text{Re } \Sigma_{TTT}^{(2)R} J_0^T \int_0^{Z_0} d\epsilon_1 \int_0^{Z_0} d\epsilon_2 \ln \frac{D}{\epsilon} \quad (\text{A.15})$$

The threshold character of relaxation determined by the Fermi golden rule is the source of asymmetry in broadening of triplet line (see the text). Now we turn to calculation of the third order diagrams ⁽³⁾ shown in Fig. 5c,d.

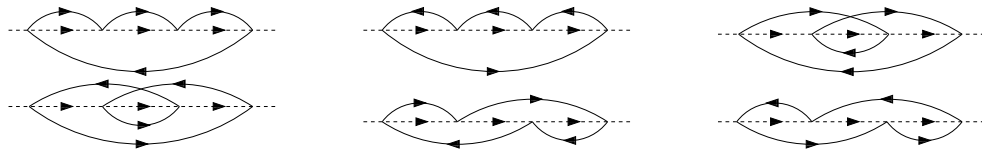


FIG. 6: Fourth order leading diagrams (a-f) for triplet self-energy part.

$$^{(3c)}(i!_n) = J^3 T^3 \sum_{!_{1,2,3}} \sum_{k_{1,2,3}} G^0(i!_1; k_1) G^0(i!_2; k_2) G^0(i!_3; k_3) G^0(i!_n + i!_1 + i!_2) G^0(i!_n + i!_2 + i!_3)$$

$$^{(3d)}(i!_n) = J^3 T^3 \sum_{!_{1,2,3}} \sum_{k_{1,2,3}} G^0(i!_1; k_1) G^0(i!_2; k_2) G^0(i!_3; k_3) G^0(i!_n + i!_1 + i!_2) G^0(i!_n + i!_2 + i!_3)$$

Evaluation of Matsubara sums gives

$$^{(3c)}(i!_n) = (J^3)^3 \sum_D \sum_D \sum_D \frac{n(2)(1 - n(1))(1 - n(3))}{(i!_n + 2)_3 (i!_n + 2)_1 (i!_n + 2)_2} \quad (A.16)$$

$$^{(3d)}(i!_n) = (J^3)^3 \sum_D \sum_D \sum_D \frac{n(1)n(3)(1 - n(2))}{(i!_n + 3)_2 (i!_n + 1)_1 (i!_n + 2)_2} \quad (A.17)$$

Let us consider first the case $\epsilon_1 = \epsilon_2 = \epsilon_3 = 0$ which corresponds to two singlet fermionic lines inserted in self-energy part. Analytical continuation leads to following expression for $\chi^{(3)} = \chi^{(3b)} + \chi^{(3c)}$ at $T = 0$:

$$\text{Im } \chi_{TSST}^{(3)}(i!) = J^{ST} \sum_D^3 \frac{J^S}{J^{ST}} \ln \frac{D}{i!} \quad (A.18)$$

$$\text{Re } \chi_{TSST}^{(3)}(i!) = J^{ST} \sum_D^3 \frac{J^S}{J^{ST}} \text{Re Li}_2 \frac{D}{i!}$$

$$\frac{J}{D} \sum_D^3 \ln^2 \frac{D}{i!} \quad (A.19)$$

where $\text{Li}_2(x)$ is a di-logarithm function⁴⁰. As we already noticed, the first log correction to $\text{Im } \chi$ appears only in 3-rd order of the perturbation theory. Thus,

$$\text{Im } \chi_{TSST}(i!) = J^{ST} \sum_D^2 \ln \frac{D}{i!} + a J^S \ln \frac{D}{i!} + \dots \quad (A.20)$$

$$\text{Re } \chi_{TSST}(i!) = J^{ST} \sum_D^2 \ln^2 \frac{D}{i!} + b J^S \ln \frac{D}{i!} + \dots + c(i!) \ln \frac{D}{i!} + d J^S \ln \frac{D}{i!} + \dots \quad (A.21)$$

with coefficient $a; b; c; d = 1$. This reproduces results of Abrikosov-Migdal theory³⁹.

We assume now that $\epsilon_1 = \epsilon_2 = \epsilon_T = 0$. It corresponds to the situation when both internal semi-fermionic GF

correspond to different components of the triplet. Following the same routine as for calculation of $\text{Im } \chi_{TTT}^{(3)}(\omega)$ we find

$$\text{Im } \chi_{TTT}^{(3)}(\omega) = J^T{}^3(\omega) \ln \frac{D}{\omega} \quad (\omega < D) \quad (\omega > D) \quad (\text{A } 22)$$

Thus, the corrections to the relaxation rate associated with transitions between different components of the triplet have a threshold character determined by the energy conservation.

Finally, we consider a possibility when two internal semi-fermionic GF correspond to different states, e.g. $\omega_1 = \omega_s = 0$, whereas $\omega_2 = \omega_T = D$. Performing the calculations, one finds

$$\text{Im } \chi_{TST}^{(3)}(\omega) = J^{ST}{}^3 \frac{J^T}{J^{ST}} \ln \frac{D}{\omega} \quad (\omega < D) \ln \frac{D}{\omega} \quad (\omega > D) + \ln \frac{D}{\omega} \quad (\omega < D) \ln \frac{D}{\omega} \quad (\omega > D) \quad (\text{A } 23)$$

Similar expression can be derived for $\text{Im } \chi_{TST}^{(3)}(\omega)$.

Any insertion of the triplet line in diagrams Fig. 5.(a-d) results in additional suppression of corresponding contribution for $\omega < D$, which, in turn, prevents the effective renormalization of the vertex J^S in contrast to the processes shown in Fig. 3. The leading correc-

tions in the 4-th order of perturbation theory are shown on Fig. 6a-f. We point out that all corrections to $\text{Im } \chi_{TTT}^{(n-2)}(\omega) \ln^2(\omega/D)$, $\text{Re } \chi_{TTT}^{(n-2)}(\omega) \ln^2(\omega/D)$ and contain an additional power of the small parameter $\omega/D \ll 1$ as $\omega \ll D$.

- ¹ L.I. Glazman and M.E. Raikh, JETP Lett. 47, 452, (1988).
- ² T.K. Ng and P.A. Lee, Phys. Rev. Lett. 61, 1768 (1988).
- ³ D.G. Oldhaber-Gordon, J.G.ores, M.A.K. astner, H. Shtrikman, D.M. ahali, and U.M. eirav, Phys. Rev. Lett. 81, 5225 (1998).
- ⁴ S.M. Cronenwett, T.H. Oosterkamp, and L.P. Kouwenhoven, Science, 281, 540 (1998).
- ⁵ F. Simmel, R.H. Blick, J.P. Kotthaus, W. Wegscheider, and M. Bichler, Phys. Rev. Lett. 83, 804 (1999).
- ⁶ T.K. Ng, Phys. Rev. Lett. 76, 487 (1996).
- ⁷ M.H. Hettler, J. Kroha, and S. Hershfeld, Phys. Rev. B 58, 5649 (1998).
- ⁸ Y. Goldin and Y. Avishai, Phys. Rev. Lett. 81, 5394 (1998), Phys. Rev. B 61, 16750 (2000).
- ⁹ A.K.aminski, Yu.V. Nazarov, and L.I. Glazman, Phys. Rev. B 62, 8154 (2000);
- ¹⁰ R. Lopez, R. Aguado, G. Platero, and C. Tejedor, Phys. Rev. B 64, 075319 (2001).
- ¹¹ K.K.ikoin and Y. Avishai, Phys. Rev. B 62, 4647 (2000);
- ¹² T.V. Shahbazyan, I.E. Perakis, and M.E. Raikh, Phys. Rev. Lett., 84, 5896 (2000).
- ¹³ T. Fujii and N. Kawakami, Phys. Rev. B 63, 064414 (2001).
- ¹⁴ K.K.ikoin and Y. Avishai, Phys. Rev. B 65, 115329 (2002).
- ¹⁵ K.K.ikoin and Y. Avishai, Phys. Rev. Lett. 86, 2090 (2001).
- ¹⁶ Y. Takazawa, Y. Imai and N. Kawakami, J. Phys. Soc. Jpn, 71, 2234 (2002).
- ¹⁷ W. Izumida, O. Sakai and Y. Shimizu, J. Phys. Soc. Jpn, 67 2444 (1998);
- ¹⁸ W. Hofstetter and H. Schoeller, Phys. Rev. Lett. 88, 016803 (2002).
- ¹⁹ M. Pustilnik, Y. Avishai, and K.K.ikoin, Phys. Rev. Lett. 84, 1756 (2000).
- ²⁰ M. Eto and Yu. Nazarov, Phys. Rev. Lett. 85, 1306 (2000), Phys. Rev. B 64, 085322 (2001).
- ²¹ D. Giuliano, B. Jouault, and A. Tagliacozzo, Phys. Rev. B 63, 125318 (2001).
- ²² M. Pustilnik and L.I. Glazman, Phys. Rev. Lett. 85, 2993 (2000), Phys. Rev. B 64, 045328 (2001).
- ²³ S. Sasaki, S. De Franceschi, J.M. Elzerman, W.G. van der Wiel, M. Eto, S. Tarucha, L.P. Kouwenhoven, Nature 405, 764 (2000).
- ²⁴ J. Nygard, D.H. Cobden, P.E. Lindelof, Nature 408, 342 (2000).
- ²⁵ W.G. van der Wiel, S. De Franceschi, J.M. Elzerman, S. Tarucha, L.P. Kouwenhoven, J. Motohisa, F. Nakajima, and T. Fukui, Phys. Rev. Lett. 126803 (2002).
- ²⁶ Y. Meir and N.S. Wingreen, Phys. Rev. Lett. 68, 2512 (1992), Phys. Rev. B 49, 11040 (1994).
- ²⁷ A. Rosch, J. Kroha, and P. Wölfe, Phys. Rev. Lett., 87, 156802 (2001).
- ²⁸ A. Rosch, J. Paaske, J. Kroha, and P. Wölfe, Phys. Rev. Lett. 90, 076804 (2003).
- ²⁹ O. Parcollet and C. Hooley, Phys. Rev. B 66, 085315 (2002), P. Coleman and W. Mao, cond-mat/0203001, cond-

- mat/0205004.
- ³⁰ L. W. Molenkamp, K. Flensberg, and M. Kemmerink, Phys. Rev. Lett. 75, 4282 (1995).
 - ³¹ A. C. Hewson, The Kondo Problem to Heavy Fermions (Cambridge University Press, Cambridge, 1993).
 - ³² V. N. Popov and S. A. Fedotov, Sov. Phys. JETP 67, 535 (1988).
 - ³³ M. N. Kiselev and R. Oppermann, Phys. Rev. Lett 85, 5631 (2000).
 - ³⁴ M. N. Kiselev, H. Feldmann, and R. Oppermann, Eur. Phys. J B 22, 53 (2001).
 - ³⁵ B. A. Jones and C. M. Varma, Phys. Rev. B 40, 324 (1989).
 - ³⁶ Possibility of additional Kondo peaks at $eV \approx T_K$ in strong magnetic field was noticed also in papers of Ref. [18], [21].
 - ³⁷ A. Kaminski, Yu. V. Nazarov, and L. I. Glazman, Phys. Rev. Lett 83, 384 (1999).
 - ³⁸ A. Abrikosov, Physics 2, 21 (1965).
 - ³⁹ A. A. Abrikosov and A. A. Migdal, J. Low Temp. Phys. 5, 519 (1970).
 - ⁴⁰ M. Abramowitz and I. Stegun, Handbook of mathematical functions. (Dover Publications, New York, 1965).